RSC Advances

Atomic Force Microscopy for Dynamic Observation of Human Erythrocytes in a Microfluidic System

Journal:	*RSC Advances*
Manuscript ID	RA-ART-09-2015-017864.R2
Article Type:	Paper
Date Submitted by the Author:	10-Nov-2015
Complete List of Authors:	Kuo, Feng-Jia; National Chung Hsing University, Physics Ho, Mon-Shu; National Chung Hsing University, Dai, Jane; National Chung Hsin University, Chemistry Fan, Ming-Huisung; National Chung Hsing University, Physics
Subject area & keyword:	Nanomaterials - Nanoscience < Nanoscience

*Submitted to **RSC Advances***

Atomic Force Microscopy for Dynamic Observation of Human Erythrocytes in a Microfluidic System

Feng-Jia Kuo[1], Mon-Shu Ho*[1, 2], Jane Dai[2] and Ming-Huisung Fan[1],

[1]Department of Physics, National Chung Hsing University, Taichung 402, Taiwan

[2]Institutes of Nanoscience, National Chung Hsing University, Taichung 402, Taiwan

Key points: A platform for rapid and effective medicine testing with AFM

Abstract

This study investigate the possibility of using atomic force microscopy (AFM) as a drug delivery system as well as a means to manipulate individual cells in an open microfluidic system for the rapid evaluation of human erythrocyte pathology in-situ. We also examined the stability and biocompatibility of a patterned polydimethylsiloxane (PDMS) platform for use in conjunction with AFM. Our results demonstrate the effectiveness of integrating a microfluidic actuator with AFM technology to conduct in-vitro medical analysis using only a miniscule quantity of human tissue.

Keywords: AFM, erythrocyte, PDMS, dynamics

I. Introduction

Microfluidic technology has attracted considerable attention as an alternative approach to rapid chemical testing in the detection of biomedical threats. Small-scale bioreactors have numerous advantages over their large-scale counterparts, including reduced processing times, lower costs, increased efficiency, and enhanced portability. These devices integrate fluidics with genomic and proteomic assays and can also be applied to chemical defense systems, clinical analysis, drug screening, and the biomedical devices used in tissue engineering. Advances in these areas have fueled the development of soft lithography technology to facilitate the fabrication of micro-pumps, micro-valves, and micro-mixers [1]. Recent developments have even led to the application of microfluidic systems in cell-based drug testing. This technology has reached higher levels of sophistication through the active control of geometry [2].

Human blood consists mainly of leukocytes, platelets, and erythrocytes. The hemoglobin proteins contained in erythrocytes are responsible for carrying oxygen from the lungs to tissue and facilitating the removal of carbon dioxide from the body via metabolism. The cytoskeleton of erythrocytes plays an important role in cellular processes such as adhesion, motility, deformation, response, and gas transportation through blood vessels [3-6]. The interfacial interactions and dynamics of erythrocytes in organisms are critical to cell physiology. These interactions have been widely investigated at the micro-scale; however, a comprehensive understanding of the mechanisms underlying the cellular dynamics remains elusive.

Atomic force microscopy (AFM) involves the use of a small probe to measure local characteristics among cells, proteins, and peptides. AFM techniques are predicated on the fact that, at the nano-scale, stretching influences traction forces under physiological conditions [7-8]. In the current study, we present an open microfluidic platform based on polydimethylsiloxane (PDMS) for the analysis of human erythrocytes using an AFM. Specifically, AFM is used to measure the stiffness of erythrocyte membranes known to present a variety of bullet-shaped deformations within blood vessels. Our results demonstrate the efficacy of using AFM to manipulate individual cells in narrow passages. To evaluate the effectiveness of the proposed microfluidic system when operated in conjunction with AFM, we investigated the response of erythrocytes to dilute sulfuric acid [9-10].

II. Methods

This study employed soft-lithography techniques for the creation of patterns used

in microfluidic systems. Electron beam lithography was used to fabricate GaAs basal plates for molding the PDMS at submicron scale while photolithography was used for imprinting the PDMS at the micron scale.

The test chip was first washed by sonication in acetone for 10 mins followed by sonication in methanol for 10 mins before undergoing sonication in DI water for 10 mins to remove unwanted particulate matter. The chip was then rinsed 3-5 times with DI water and blow-dried using nitrogen gas before being heated to 150 °C to evaporate any remaining water from the surface. A photo-resistive layer of PMMA was applied to the cleaned glass chip. Centrifugation was applied at 1500 rpm for 30 s before being increased to 2500 rpm for 1 s then soft-baked at 80 °C for 5 mins. Note that considerable trial and error was required to find the most suitable combination of techniques. A mask was placed on the PMMA-coated chip and subjected to UV light. Removal of the exposed areas was achieved by soaking in methyl-isobutyl ketone and IPA at a ratio of 1:3 for 75 s at a constant temperature of 30 °C followed by placement in pure IPA for 25 s. The chip underwent two sessions of soaking in DI water for 30 s and blow-dried with nitrogen gas. It was then hard-baked at 150 °C for 80 s. The chip was subjected to wet anisotropic etching through soaking in a solution of sulphuric acid, hydrogen peroxide, and water in the ratio of 1:8:40 for 30 s, which resulted in an etching depth of 500nm. The chip was rinsed continuously in ultrasonic cleaner for 3-5 mins and then dried under nitrogen gas. PDMS provided by Dow Corning Corporation was mixed with a curing agent using a stirring rod at a ratio of 10:1 until bubbles formed. This mixture was then held under low vacuum for 30-40 mins, until all of the bubbles were visibly removed. The PDMS/curing agent mixture was layered over the patterned chip and soft-baked at 70 °C for 30 mins. After the PDMS mixture had solidified, it was removed from the chip.

The interactions between human erythrocytes and the PDMS substrate were examined using AFM (Brucker, Dimension 3100) by observing cells under sodium chloride physiological conditions in an aqueous environment. The AFM experiments were conducted using V-shaped Si_3N_4 cantilevers with a tip radius of 10-25nm, aspect ratio of 1:1, resonance frequency of 7-120 kHz, and a spring constant of approximately 0.9 to 0.12N/m. Images showing the topography of the substrate were obtained using AFM in tapping mode. Contact mode and Quantitative Nano Mechanics (QNM) mode measurements were used to determine the adhesion of cell membranes. The parameters used in the AFM experiments are as follows: scanning rate of 0.3-0.5kHz in liquid as well as in air, and retraction speed of approximately 1kHz. Step motor moves 0.400um per step. During scanning, the maximum Z-range was set to 12um and the height was set to 150nm. For tapping mode scanning, we used resonance frequencies of 10-30Hz in liquid and 500-700Hz in air.

The dynamics of human erythrocytes in microfluidic systems was investigated through a series of steps. We first moved a red blood cell (RBC) by inducing capillary action via the placement of a dust-free wipe (Kimberly Clark Professionals) at the outlet to absorb the liquid within. The movement of the liquid medium dragged the RBC with it. Closing off one of the outlets forced the RBC to move into the other outlet, whereupon it was "pushed" toward the exit using AFM via atomic manipulation. Finally, cell destruction of the RBC was monitored after it entered the cavity by adding sulphuric acid (Concentration).

Blood was obtained by pricking a finger. One drop of blood was obtained by the pricking of a finger under medical supervision after obtaining the informed consent of the participants [11]. To every 3mL of blood was added 5.4mg of ethylenediaminetetraacetic acid (EDTA) to prevent clotting. The blood was then added to phosphate buffer solution (PBS) (Sigma Aldrich) at a dilution of 1:100. The mixture was centrifuged to obtain high concentrations of erythrocytes and subsequently diluted by a factor of 100,000 using physiological saline solution at 4^{o}C. Fig. 1 presents a flow chart illustrating the process used in RBC preparation.

An evaporator was used to treat the patterned PDMS substrate with poly-L-lysine and glutaraldehyde solutions prior to the dropwise addition of the erythrocyte mixture on to the patterned PDMS substrate [12-13]. The gluteraldehyde also led to the calcification of the surface cytoskeleton of the erythrocyte membrane, which reduced the likelihood that the membrane of the erythrocyte would be pierced by the AFM tip during measurements to obtain the force curve.

A glass chip was cut to 2cm x 2cm, and secured to the glass slide using double-sided tape. Using sellotape, a single layer of mica was carefully removed from the top. Poly-L-Lysine (0.01% w/v) was added to the mica drop-wise until it was entirely covered, whereupon it was heated to 30°C and held for an hour before being gently rinsed using 200mL DI water.

The roughness values (Ra-value) of clean and treated PDMS surfaces were 0.5nm and 1nm, respectively. Phosphate buffer solution was used to remove excess erythrocytes from the PDMS surface and serve as a carrying fluid. Sulfuric acid was used to test the accuracy of the analysis performed using the proposed microfluidic system. Liquid physiological conditions were maintained throughout the experiment.

III. Results and Discussion

Mica plates and PDMS are both used widely in comparative biology; however, PDMS-based materials tend to be preferred because they are easily patterned using soft-lithography techniques. This study examined human erythrocytes on mica, PDMS,

and patterned PDMS plates, each of which presented a roughness value of less than 1nm. Table I presents measurements of erythrocyte topography on each of the substrates, as determined by AFM.

The erythrocytes were concave and uniform in size. Specifically, the measured dimensions were approximately 6.2 – 7μm in diameter, 1.15 – 1.84μm in thickness, and 1.22 – 1.74μm in the depth of the cell sink. The small variations in these measurements may be attributed to differences in the interactions between the surface of the substrate and the erythrocytes. The PDMS was patterned as an erythrocyte container with hollow squares measuring 10μm x 10μm. Each well was only 1μm in height (Fig. 5) to prevent the erythrocyte mixture from flooding during dynamic AFM observation in an aqueous environment. The resulting patterns were carefully checked to ensure that they had altered the appearance of the erythrocytes only slightly. The stiffness of the cell membrane on each substrate was also examined using adhesion force measurements obtained by AFM. The adhesion force in erythrocyte protrusions was approximately 4.20±0.70nN on mica, 5.00±1.50nN on PDMS, and 4.60±0.80nN on patterned PDMS. The adhesion force in erythrocyte sinks was 0.64±0.14nN on mica, 1.13±0.83nN on PDMS, and 1.10±0.53nN on patterned PDMS. Fig. 2 presents the histograms for the adhesion of RBC cells on mica and PDMS substrates. T-tests presented P-values of only 0.016 for the bulging side of the RBC cells and $2.4X10^{-9}$ for the center of the cells. The test results indicate that the selection of substrate has notable effects on the nanomechanical measurements of the cells they support. These measurements are important because the adhesion of the erythrocyte to the surface of the substrate is proportional to the value of the force curve. The sunken centers of the erythrocytes have a smaller adhesion force (similar to that of hard-textured materials) compared to that of the erythrocyte protrusions. Data obtained from adhesion measurements revealed that PDMS plates are superior to mica plates in diversifying erythrocytes. Measurements obtained on mica plates indicated that following the aggregation of internal proteins, erythrocytes were transformed from a liquid state to a soft solid state; however, the cytoskeleton of the membrane retained its flexibility. This confirms that the size of the contact area on the cell membrane to which the cells adhered could alter the fluidity of lipids by hardening the exterior of the cellular membrane, thereby reducing surface adhesion forces [14]. A number of researchers have suggested that the adhesion force between a bio-sample and the basal plate may vary according to the substrate. Basal plates with a larger traction force (e.g. mica plates) present a stronger binding force with the bottom of the erythrocyte; however,

these materials also present low surface adhesion at the upper surface of the erythrocytes. Conversely, a small binding force between the PDMS substrate and the bottom of the erythrocytes was shown to increase adhesion at the upper surface. As a result, PDMS is considered a superior choice for the investigation of cells using AFM.

Figures 3 (a) and (b) present AFM images and profile analysis of self-assembled human erythrocytes on a PDMS plate without additional treatment. Figures 3(c) and 3(d) present examples of the force curves obtained by measuring the erythrocytes in Figs. 3(a) and 3(b). Figure 3(c) illustrates the bulging sides of the erythrocytes and 3(d) shows the concave center. The spacing between erythrocytes on PDMS plates was determined to be 8.14±0.28μm with a mean cell diameter of 7.19μm based on measurements from 50 erythrocytes. The spacing on PDMS was slightly tighter and more ordered than that observed on mica [15]. The self-assembly of erythrocytes, involving the arrangement of atoms or small molecules, was facilitated by minimal surface tension and free energy at the surface. Our observations suggest that mutual interactions among erythrocytes pull them together into a self-assembled hexagonal close-packed (HCP) structure. Our results also demonstrate that, compared to mica, PDMS is more compatible with biological organisms, which make it ideal for use as a basal plate in bio-sample research.

Atomic force microscopy (AFM) enables atoms and small molecules to be manipulated on substrate surfaces [16]. This effect also pertains to nano-scale operations associated with atomic migration, cell membrane electroporation, and chromosome dissection at the molecular level [17]. This study further demonstrated the applicability of AFM in the manipulation of macromolecules, such as erythrocytes, in an aqueous environment. The contact mode along with “peak force” software in Brucker-AFM was applied to maintain careful control over the applied force and speed, thereby ensuring that every movement was tiny. The program controls the AFM hardware to produce movements of 10-30nm staring with 100pN in every step, and then the value is adjusted thereafter to 10nN on the PDMS. As shown in Figs. 4(a) and 4(b), moving erythrocytes on the PDMS substrate using an AFM tip did not damage or distort the samples. These results demonstrate the effectiveness of employing a PDMS substrate in conjunction with AFM technology to determine the specific location of erythrocytes in samples for advanced experimentation [18-19].

We employed a nano-imprinting technique based on soft lithography to create a pattern of squares (10μm×10μm) on the PDMS plates in order to reduce the possibility of fluid flooding during medical analysis using AFM on a PDMS substrate. Optical

microscopic (OM) images illustrate a well-aligned array fabricated using this method. The protrusions making up the squares were approximately 2μm in width and 500nm in height, which is roughly half the height of the erythrocytes. Surplus erythrocytes were removed from the patterned PDMS by washing with PBS, such that the remaining erythrocytes were held within the indentions. This made it possible to re-examine the shape and characteristics of the erythrocytes within this aqueous environment. The differences in AFM topography were negligible, which implies that this patterned PDMS substrate is highly suitable for this type of research.

This study examined the medical response of erythrocytes to sulfuric acid as a manifestation of the metabolism of steroids and associated interactions [20]. The acid was well-mixed with PBS prior to application via pin-hole injection. AFM was then used to observe the influence of the external environment on the erythrocytes in-situ. Figures 5(a)-(c) present AFM images showing the topography and phase of an erythrocyte on patterned PDMS, taken before [5(a)], during [5(b)], and after [5(c)] the sample was flooded with 20μl of the sulfuric acid mixture. These images clearly demonstrate the ability of the patterned PDMS to secure cells within patterned PDMS sinks, despite the presence of wave-generated noise created by the addition of sulfuric acid solution. The addition of the sulfuric acid mixture altered the osmotic pressure of the buffering solution, which in turn caused the erythrocytes to burst. The released cytoplasm was carried away by the flow. The AFM phase diagram in Fig. 5(c) clearly shows burst erythrocytes on a patterned PDMS plate, even though the topography image of the erythrocyte is not particularly clear. These results demonstrate the applicability of PDMS in the creation of a chemical-free basal plate and the effectiveness of using AFM to facilitate the observation of cells in-situ.

In this study, we designed substrates with pipe-like patterns and small holes [Fig. 6(a)] to serve as a microfluidic drug delivery system and simulate the mobility of erythrocytes in capillaries. The high degree of elasticity in the treated erythrocytes enabled cell deformation and recovery while traveling through narrow passages, as shown in Fig. 6(b). The passages were approximately 10μm and 30μm wide for high flow rates and 3μm, 5μm and 7μm for low flow rates. The flow of erythrocytes could be controlled in two ways. To achieve a high flow rate, capillarity could be applied using pin-hole injection at one end and air-laid paper absorption at the other. This caused the solution to flow, which in turn drove the movement of the erythrocytes. As shown in Fig. 7(a), a low flow rate could be achieved using AFM manipulation, wherein individual erythrocytes are led toward a small opening, followed by the injection of sulfuric acid

solution through the microfluidic system. Figure 7(b) illustrates erythrocyte hemolysis with the subsequent overflow of cytoplasm. Figure 7(c) shows residual cytoplasm drifting away in the fluid. These findings demonstrate the efficacy of using AFM to record instantaneous responses in individual molecules.

In hydrodynamics, fluid pressure is inversely correlated with fluid speed. The small holes in this experiment served as pumps capable of generating a driving force when flow crossed various areas of the passages. Flow could be paused when erythrocytes were directed through narrow passages, in order to facilitate the measurement of adhesion to cell membranes. The force curves in Fig. 8 illustrate how changes in the shape of the erythrocytes also change the shape of the force curve. This means that different substrates could alter the shape of the erythrocyte, thereby altering its force curve, depending on the strength of the adhesion force between the erythrocytes. The measured adhesion values obtained from erythrocyte sinks were 2.00±0.45nN, 0.64±0.19nN and 0.22±0.07nN in passages with widths of 7μm, 5μm and 3μm, respectively. The measured adhesion values obtained from erythrocyte protrusions were 3.74±0.29nN, 1.5±0.24nN and 0.96±0.26nN in passages with widths of 7μm, 5μm and 3μm, respectively. These results demonstrate that the adhesion of cell membranes decreased with an increase in erythrocyte deformation in narrow passages. These observations further imply that the cytoskeleton of the membrane assembled in the form of concentered structures. Concentered structures combined with a lack of flexibility in erythrocytes could result in serious pathological conditions and thrombotic diseases.

IV. Conclusions

This study developed an open microfluidic system capable of rated-programming, activation-modulation, and site-targeting for the testing of drug delivery systems. Our findings demonstrate that the inherent stability and biocompatibility of patterned PDMS materials enables them to preserve the original features of cells. In other words, the erythrocytes have less attractive force when placed on a PDMS surface than when placed on mica. Thus, the adhesion of the cell to the PDMS substrate is insufficient for the cell to become distorted, as is the case with mica. The results obtained from a PDMS micro-fluidic system closely mimic the free-flowing erythrocytes within the blood stream, which does not interact with the walls of the blood stream. The fact that the erythrocytes do not adhere to the walls of blood vessels may also be due to the force at which the blood is pumped throughout the body, thereby depriving the erythrocytes of

sufficient time to interact in a manner that would allow the concave portion of the cell to contact the surface of the blood vessel. Moreover, AFM can be used to facilitate the manipulation of individual human erythrocyte cells in order to measure adhesion and record reactions of cells to the release of drugs at specific sites. The proposed system provides a highly efficient platform for the rapid evaluation of erythrocyte pathology in-situ.

Table 1 : Characteristics of human erythrocytes on mica, PDMS, and patterned PDMS substrates

	Mica	PDMS	Patterned PDMS
Cell diameter	**6.94±0.43µm**	**7.19±0.53µm**	**7.11±1.24µm**
Cell thickness	**1.84±0.15µm**	**1.50±0.15µm**	**1.35±0.05µm**
Cell depression	**1.22±0.49µm**	**1.74±0.20µm**	**1.26±0.08µm**
Adhesion force measured at cell protrusions	**4.20±0.70(nN)**	**5.00±1.50(nN)**	**4.60±0.80(nN)**
Adhesion force measured at cell sinks	**0.64±0.14(nN)**	**1.13±0.83(nN)**	**1.10±0.53(nN)**

Table 1. Characteristics of human erythrocytes on mica, PDMS, and patterned PDMS substrates

Figure Captions:

Fig. 1 Flow chart of process used in preparation of human red blood cells for AFM measurement

Fig. 2 Histograms for the adhesion of RBC cells on mica and PDMS substrates

Fig. 3 (a): AFM images and line profiles indicating self-assembly of erythrocytes on a PDMS substrate without the need for additional treatment. As shown by the dotted lines, under the right conditions, erythrocytes will undergo self-assembly of hexagonal close packing; (b) profile analysis for Fig.1 (a) showing cell diameter of 6.2~7 μm, thickness of 1.15~1.84 μm, and cell sink depth of 1.22~1.74 μm (blue and red lines separately indicate the topology of individual erythrocytes); (c) and (d) force curves obtained from erythrocyte protrusions and sinks, respectively with spacing of 8.14±0.28μm between erythrocytes and the PDMS plates and a mean cell diameter of approximately 7.19μm.

Fig. 4 (a) Erythrocytes A, B, and C before being shifted using an AFM tip; (b) erythrocytes A, B, and C after being shifted on the PDMS substrate. The arrows indicate the direction in which the force was applied by the AFM tip.

Fig. 5 AFM image of human erythrocytes aligned within 10μm x 10μm squares set into PDMS plates. The walls separating the squares are approximately 0.5μm in height: (a) image obtained before sample was flooded with 20μL of H_2SO_4 (aq); (b) during flooding of sample; and (c) after flooding of sample. Figures (d) to (f) present phase diagrams of Figs. (a) to (c) respectively. Comparing the topographic image in (c) to its phase equivalent in (f) reveals a semblance of an erythrocyte that in (f) would not otherwise be detectable in (c). This observation is a clear indication that the erythrocyte burst.

Fig. 6 (a) Dynamic observation of human erythrocytes in the proposed microfluidic drug delivery system; (b) enlarged image of (a) showing that erythrocytes are able to pass through passages that are smaller than their diameter via shape deformation.

Fig. 7 AFM evaluation of drug delivery system: (a) erythrocytes moved to specific destination via AFM manipulation. This movement simulates a low flow rate in the system; (b) hemolysis of erythrocytes following the addition of H_2SO_4 (aq.); and (c) residual cytoplasm drifting away in the fluid following the completion of hemolysis.

Fig. 8 AFM images of deformed human erythrocytes in microfluidic system: (a) passage width of 7μm with force curve showing adhesion force of erythrocyte sink (below 2.00±0.45nN) and erythrocyte protrusion (3.74±0.29nN); (b) passage width of 5μm with force curve showing adhesion force of erythrocyte sink (below 0.64±0.19nN) and erythrocyte protrusion (1.5±0.24nN); and (c) passage width of 3μm with force curve showing adhesion force of erythrocyte sink (below 0.22±0.07nN) and erythrocyte protrusion (0.96±0.26nN).

Acknowledgements

The authors would like to thank the Ministry of Science and Technology of the Republic of China, Taiwan, for their financial support in this research, under Contract No. NSC102-2112-M-005-003-MY3. The ideas, results and conclusion in no way reflect the opinion of the Ministry of Science and Technology of the Republic of China, Taiwan. The authors also want to express their sincere thanks to Prof. Duen-Yau Chuang, Professor in Department of Biochemistry at National Chung Hsing University, for discussion in cell biology.

Contribution: M.S. Ho designed the research and wrote the paper; F.J. Kuo, and M.H. Fan performed experiments; F.J. Kuo analyzed AFM results and M.H. Fan analyzed microfluid results. Jane Dia revised the paper. M.S. Ho made the figures.

Conflict-of-interest disclosure: The authors declare no competing.

Corresponding*

Mon-Shu Ho, Professor in Department of Physics and institute of Nanoscience, National Chung Hsing University, 250 Kuo-Kuang Rd., Taichung 40227, Taiwan

Email: msho@dragon.nchu.edu.tw

Tel: +886-4-22840427 ext 519

Fax: +886-4-22862534

References:

[1] Dong Qin, Younan Xia and George M Whitesides, "Soft lithography for micro- and nanoscale patterning", *Nature Protocols* **5**, - 491 - 502 (2010)

[2]Didier Falconnet, Gabor Csucs, H. Michelle Grandin, Marcus Textor, "Surface engineering approaches to micropattern surfaces for cell-base assays" Biomaterials 27 3044–3063 (2006)

[3] Gorter, E., and Grendel, F., "On biomolecular layers of lipoids on the chromocytes of the blood" J. Exp. Med., 41, 439 (1925).

[4] Denker BM, Smith BL, Kuhajda FP, Agre P, "Identification, purification, and partial characterization of a novel Mr 28,000 integral membrane protein from eryrhorcytes and renal tubules"J Biol Chem 263, 1563 (1988).

[5]R. MacKinnon and C. Miller, ibid. 245, 1382 (1989).

[6]Y.Martin and H.K.Wickramasinghe, "Magnetic imaging by“force microscopy”with 1000Å resolution"Appl. Phys. Lett. 50, 1455 (1987).

[7]Red Gold - Blood History Timeline, PBS 2002. Accessed 27 December 2007.

[8]Nowakowski R., Luckham P., Winlove P., "Imaging eryrhorcytes under physiological conditions by atomic force microscopy", Biophys.Biochem.Acta 1514, 170-176 , 2001.

[9]Luna, EJ and AL Hitt, "Cytoskeleton-plasma membrane interactions" Science 258, 955-964 (1991)

[10] McGraw Hill, "Swammerdam, Jan (1637–1680)", AccessScience, (2007)

[11] All blood drawing protocol followed and complied with the "Guidance Blood Drawing Protocol" (IRB(Institutional Review Boards) version, revised 2008), University of Vermont, Burlington, US. The blood samples were taken in accordance with the guidelines of “Patient Portal Access” at Changhua Christian Hospital, which is located at 135 Nanxiao St., Changhua City Changhua Country 500, Taiwan.

[12] H. Wang, R. Bash, J. G. Yodh, G. L. Hager, D. Lohr, and S. M. Lindsay, "Glutaraldehyde modified mica: a new surface for atomic force microscopy of chromatin. " Biophys. J. 83, 3619 (2002).

[13] S. Sen, S. Subramanian, and D. E. Discher, "Indentation and Adhesive Probing of a Cell Membrane with AFM: Theoretical Model and Experiments" Biophys. J. 89, 3203 (2005).

[14] L. Zhang and S. Granick, "Slaved Diffusion in Phospholipid Bilayers," Proc. Nat. Acad. Sci. USA 102, 9118 (2005).

[15] Mon-Shu Ho, Feng-Jia Kuo, and Yu-Siang Lee," Atomic force microscopic observation of surface-supported human erythrocytes ", Applied Physics Letter 91, 023901 (2007)

[16] Oscar Custance, Ruben Perez and Seizo Morita, " Atomic force microscopy as a tool for atom manipulation", *Nature Nanotechnology***4**, 803 - 810 (2009)

[17] Kathryn A. Melzak etc., " AFM measurements and lipid rearrangements: evidence from red blood cell shape changes " Soft Matter, 2012, 8, 7716

[18] Florin EL,Moy VT, Gaub HE, "Adhesion forces between individual ligand-receptor pairs. "Science 264,415 (1994)

[19] Parbin BC et al:Probing recognition process between an antibody and an antigen using atomic force microscopy. Physicochemical and Engineering Aspect 143, 53-57 (1998)

[20] W Schänzer, " Metabolism of anabolic androgenic steroids. "Clinical Chemistry 42, no. 7 1001-1020 (1996)

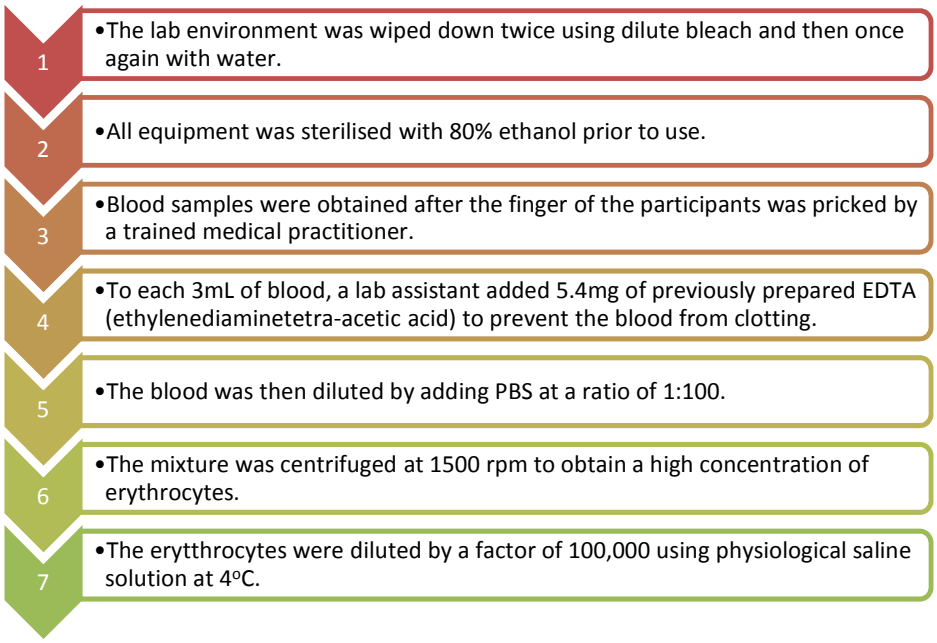

Fig. 1 Flow chart of process used in preparation of human red blood cells for AFM measurement

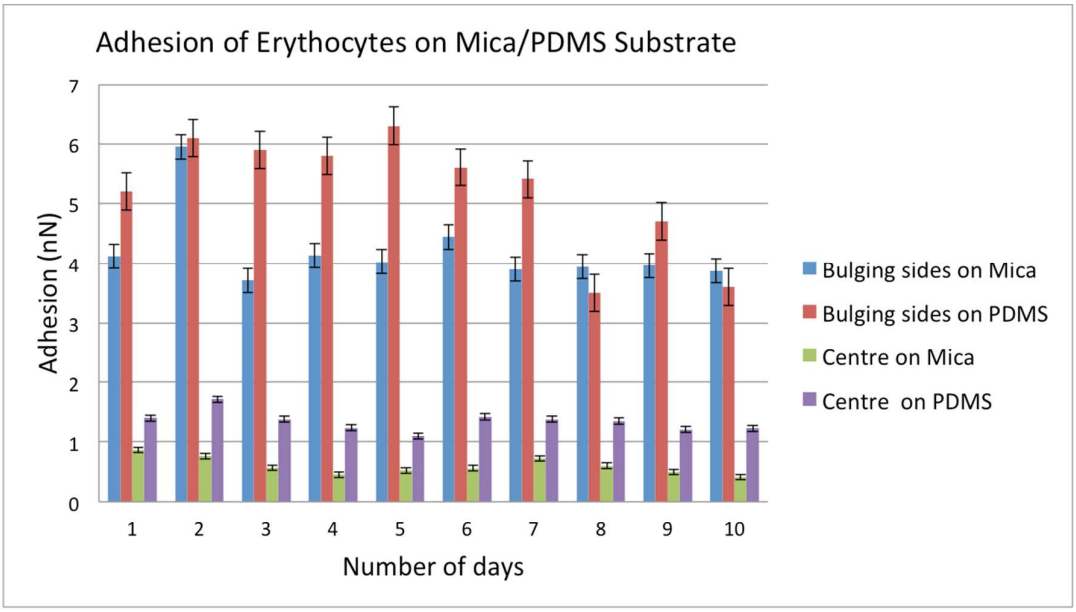

Figs. 2 Histograms for the adhesion of RBC cells on mica and PDMS substrates

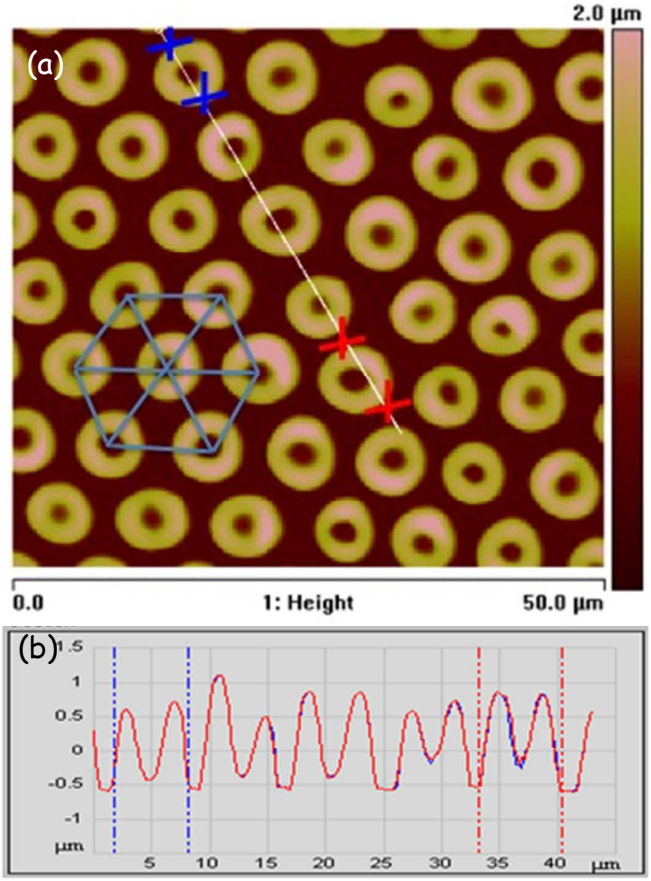

Fig. 3 (a): AFM images and line profiles indicating self-assembly of erythrocytes on a PDMS substrate without the need for additional treatment. As shown by the dotted lines, under the right conditions, erythrocytes will undergo self-assembly of hexagonal close packing; (b) profile analysis for Fig.1 (a) showing cell diameter of 6.2~7 µm, thickness of 1.15~1.84 µm, and cell sink depth of 1.22~1.74 µm (blue and red lines separately indicate the topology of individual erythrocytes); (c) and (d) force curves obtained from erythrocyte protrusions and sinks, respectively with spacing of 8.14±0.28µm between erythrocytes and the PDMS plates and a mean cell diameter of approximately 7.19µm.

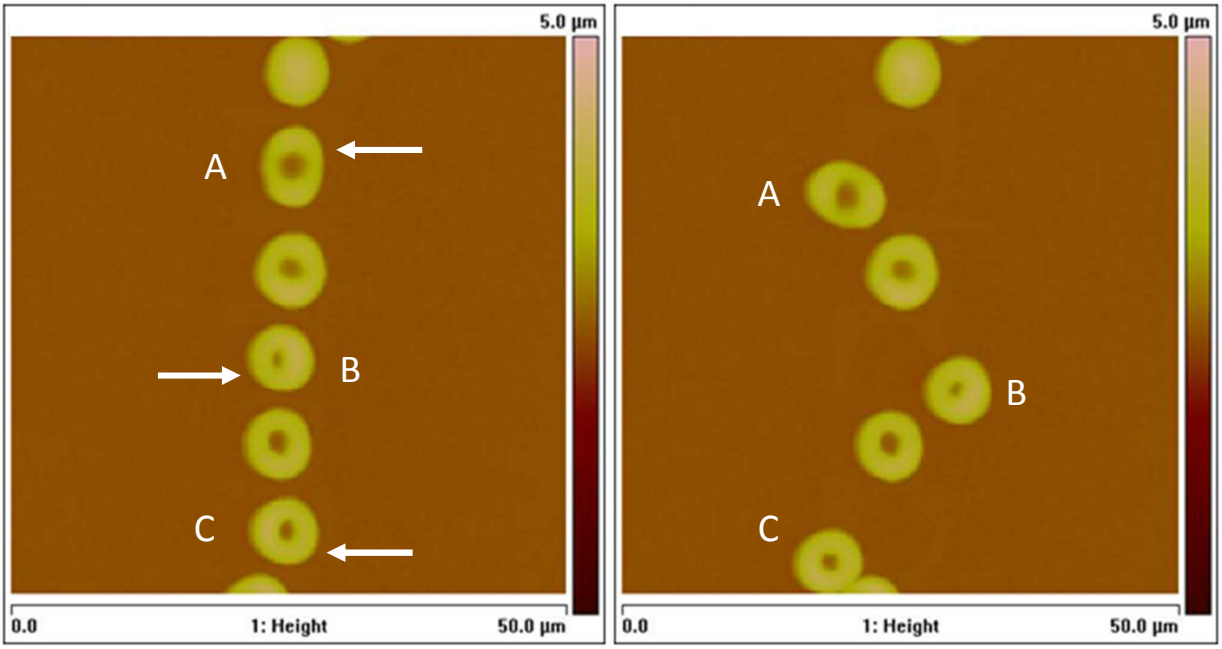

Fig. 4 (a) Erythrocytes A, B, and C before being shifted using an AFM tip; (b) erythrocytes A, B, and C after being shifted on the PDMS substrate. The arrows indicate the direction in which the force was applied by the AFM tip.

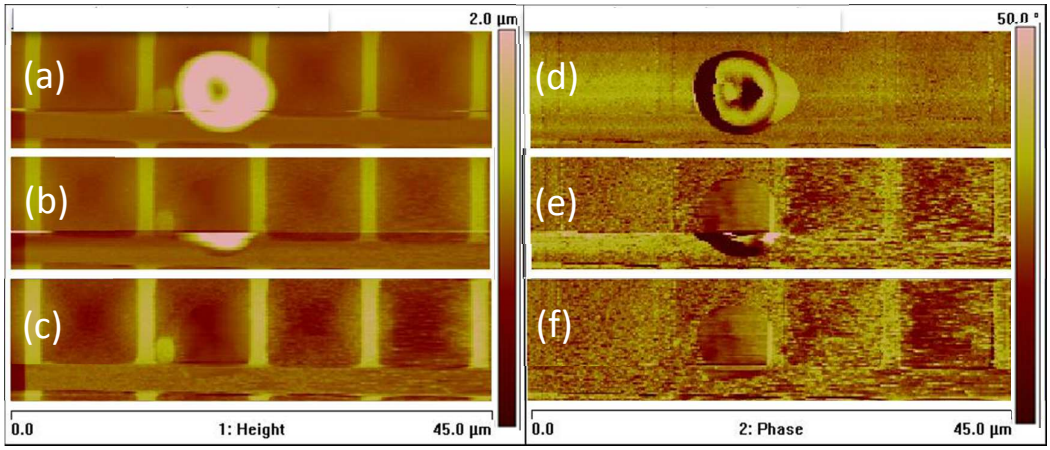

Fig. 5 AFM image of human erythrocytes aligned within 10µm x 10µm squares set into PDMS plates. The walls separating the squares are approximately 0.5µm in height: (a) image obtained before sample was flooded with 20µL of H_2SO_4 (aq); (b) during flooding of sample; and (c) after flooding of sample. Figures (d) to (f) present phase diagrams of Figs. (a) to (c) respectively. Comparing the topographic image in (c) to its phase equivalent in (f) reveals a semblance of an erythrocyte that in (f) would not otherwise be detectable in (c). This observation is a clear indication that the erythrocyte burst.

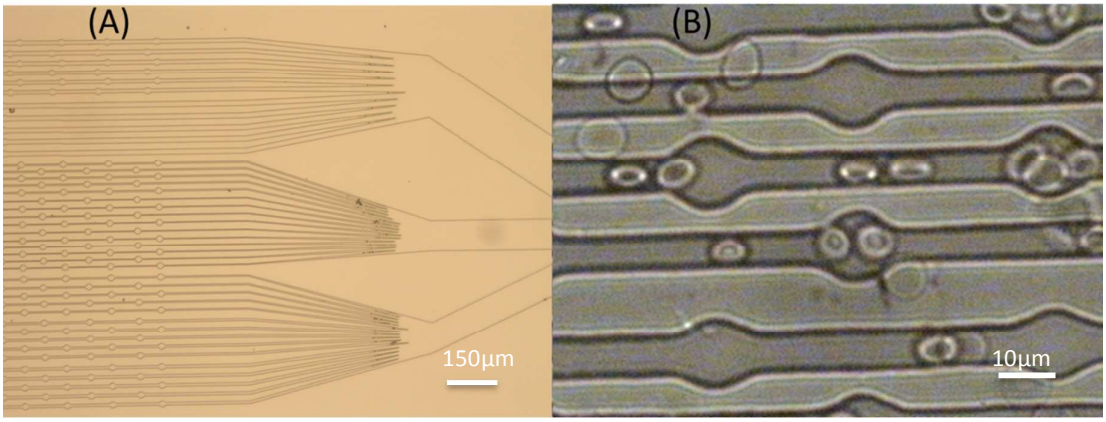

Fig. 6 (a) Dynamic observation of human erythrocytes in the proposed microfluidic drug delivery system; (b) enlarged image of (a) showing that erythrocytes are able to pass through passages that are smaller than their diameter via shape deformation.

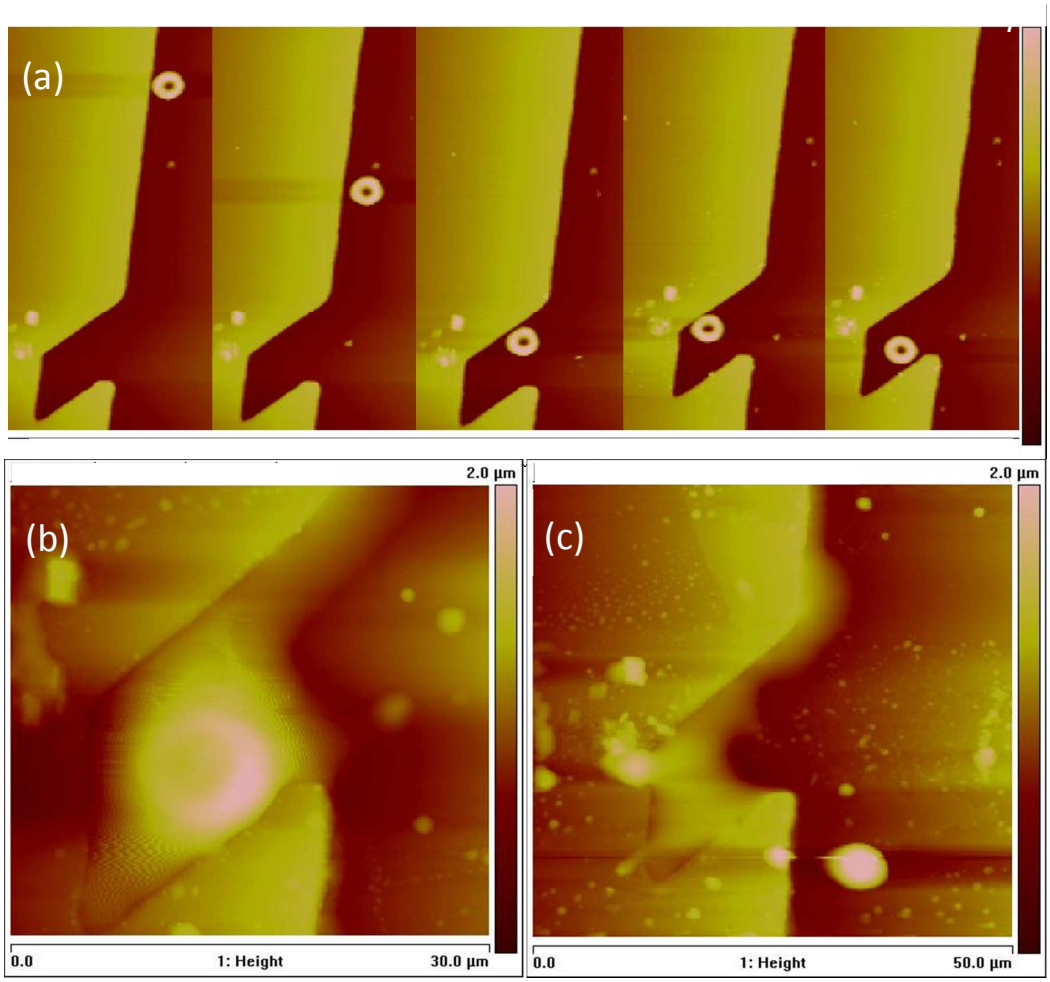

Fig. 7 AFM evaluation of drug delivery system: (a) erythrocytes moved to specific destination via AFM manipulation. This movement simulates a low flow rate in the system; (b) hemolysis of erythrocytes following the addition of H_2SO_4 (aq.); and (c) residual cytoplasm drifting away in the fluid following the completion of hemolysis.

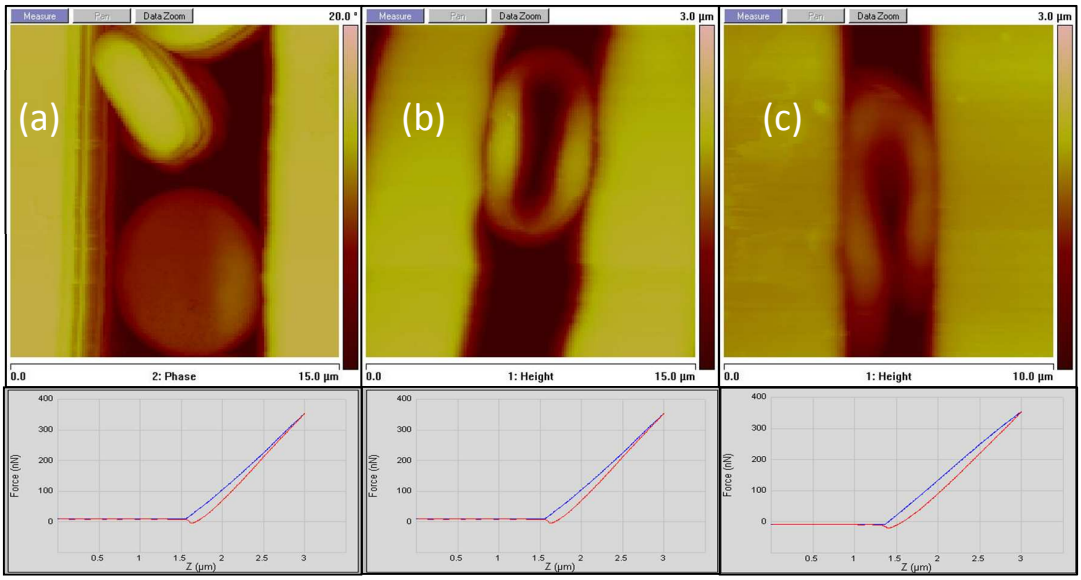

Fig. 8 AFM images of deformed human erythrocytes in microfluidic system: (a) passage width of 7µm with force curve showing adhesion force of erythrocyte sink (below 2.00±0.45nN) and erythrocyte protrusion (3.74±0.29nN); (b) passage width of 5µm with force curve showing adhesion force of erythrocyte sink (below 0.64±0.19nN) and erythrocyte protrusion (1.5±0.24nN); and (c) passage width of 3µm with force curve showing adhesion force of erythrocyte sink (below 0.22±0.07nN) and erythrocyte protrusion (0.96±0.26nN).